Plant Cell Physiol. 39(10): 1111-1118 (1998)
JSPP © 1998

Rapid Report

AGR, an *Agravitropic* Locus of *Arabidopsis thaliana*, Encodes a Novel Membrane-Protein Family Member

Kaname Utsuno, Toshiharu Shikanai, Yasuyuki Yamada and Takashi Hashimoto

Graduate School of Biological Sciences, Nara Institute of Science and Technology, Nara, 630-0101 Japan

Mutations in the *Agr* locus of *Arabidopsis thaliana* impair the root gravitropic response. Root growth of *agr* mutants is moderately resistant to ethylene and to an auxin transport inhibitor. Vertically placed *agr* roots grow into agar medium containing IAA or naphthalene-1-acetic acid, but not into medium containing 2,4-D. Positional cloning showed that *AGR* encodes a root-specific member of a novel membrane-protein family with limited homology to bacterial transporters.

Key words: *Arabidopsis thaliana* — Auxin — Ethylene — Membrane protein — Root gravitropism.

Plants sense the vector of gravity using starch-filled amyloplasts as the statolith (Sack 1991). In the root tip, amyloplasts within the columella root cap sediment in the direction of gravity initiating the root gravity response, which ultimately generates an asymmetrical auxin distribution within the elongation zone (Evans 1991). According to the Cholodny-Went hypothesis, IAA accumulates along the lower side of the elongation zone of horizontally-placed roots, and inhibits cell elongation there, thus causing the downward bending of the roots. The mechanisms that generate IAA redistribution after gravity perception are not known, but the characterization and molecular cloning of several gravitropic loci in *Arabidopsis thaliana* is a promising approach. The *agr* mutant possessing impaired root gravitropism is unique among the many abnormally gravitropic mutants because its defect is restricted to the root, yet root growth is inhibited by exogenously supplied auxin as in the wild type (Bell and Maher 1990). The *agr* columella cells also develop normal amyloplasts (unpublished observations). The *AGR* locus may thus represent a step between gravity perception and auxin redistribution in the roots. Here we report on the further characterization of the *agr* mutant and the molecular cloning of the *AGR* locus using a map-based approach.

Phenotypic characterization of five agr alleles—Since complementation tests showed that *agr* is allelic to *eir1* (Roman et al. 1995) (data not shown) and *wav6-52* (Okada and Shimura 1990), five *agr* alleles, *agr-1, agr-2, agr-3* (Bell and Maher 1990), *wav6-52*, and *eir1-1*, were phenotypically characterized. *eir1-1* is in the Columbia (Col) background, while the other alleles are in the Lansberg *erecta* (Ler) background. The root gravitropic response of the wild types and *agr* mutants was assessed by measuring curvature after gravistimulation at 135 degrees to the vertical (Fig. 1). Wild-type roots (Ler and Col) sharply responded to the change in the gravity vector, whereas the response of *agr* roots was severely impaired. The severity of the mutant phenotype was difficult to rank in a defined order, but a replicate experiment (not shown) confirmed that *agr-1* and *wav6-52* are strong alleles, while *agr-3* and *eir1-1* retain a residual gravitropic response. The gravitropic response of the stem and hypocotyl, and the phototropic response of

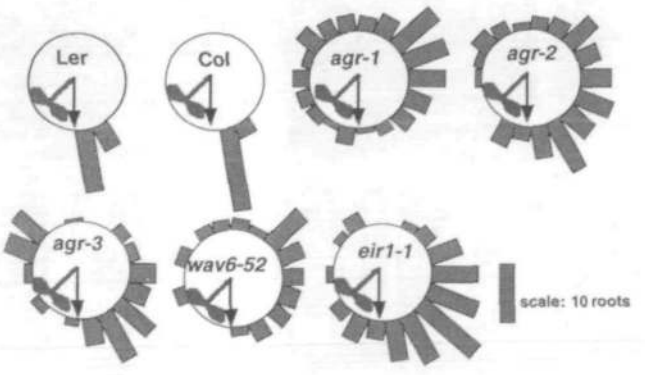

Fig. 1 Distribution of root growth directions. Wild-type and *agr* mutants were grown aseptically under continuous white light (80 μmol m^{-2} s^{-1}) on Arabidopsis mineral nutrient agar (Haughn and Somerville 1986) with 1% sucrose for 3 d at 23°C. The agar plates were then rotated to an angle of 135° and kept in the dark for one day. The angle between each root tip axis and the vertical was measured.

Abbreviations: ACC, 1-aminocyclopropane-1-carboxylic acid; CAPS, cleaved amplified polymorphic sequence; Col, Columbia; EST, expressed sequence tag; Ler, Landsberg *erecta*; NAA, naphthalene-1-acetic acid; ORF, open reading frame; RACE, rapid amplification of cDNA ends; RFLP, restriction fragment length polymorphism; RT, reverse transcription; TIBA, 2,3,5-triiodobenzoic acid, YAC, yeast artificial chromosome.

The nucleotide sequence reported in this paper has been submitted to the GenBank under accession number AF093241.

Corresponding author: Takashi Hashimoto, e-mail: hasimoto @bs.aist-nara.ac.jp

Downloaded from https://academic.oup.com/pcp/article/39/10/1111/1844994 by guest on 20 August 2022

Table 1 Root growth of wild-type and *agr* seedings

	IAA (nM)		ACC (nM)		TIBA (μM)	
	3	10	10	100	1	10
Ler	77.6±5.3	70.4±7.6	72.7± 5.7	42.1±4.1	93.6± 8.3	37.1±3.4
Col	77.4±5.8	71.2±4.9	68.6± 4.9	46.1±2.6	97.5± 7.9	40.2±5.3
agr-1	74.2±5.5	71.8±5.3	96.2± 9.4	68.0±6.0	94.6± 8.3	56.1±3.9
agr-2	76.3±4.2	68.3±4.9	94.4±12.8	73.1±7.5	108.4± 8.9	56.5±4.6
agr-3	69.3±6.0	66.7±4.6	78.2± 6.4	57.2±6.7	106.3± 7.0	53.3±5.5
wav6-52	73.0±5.2	58.6±5.3	104.5± 8.1	70.0±5.9	108.3± 8.3	59.6±5.1
eir1-1	73.1±6.2	72.8±4.5	92.3±10.5	80.5±4.7	104.0±10.1	60.1±3.4

Three-day-old seedlings grown as described in Fig. 1 were transferred onto agar medium containing IAA, ACC, or TIBA, and grown for a further 3 d. Root growth rate (mean±S.D.) was normalized to root growth on unsupplemented medium as 100%. At least four concentrations were tested for each compound, but the data from two representative concentrations are shown.

the root appeared to be normal in all five *agr* alleles (data not shown).

IAA, naphthalene-1-acetic acid (NAA), and 2,4-D inhibited root growth to the same extent in both wild types and all 5 *agr* mutants (Table 1 and data not shown). *agr* root elongation was somewhat more resistant than the wild types to 2,3,5-triiodobenzoic acid (TIBA), an inhibitor of auxin transport which inhibits cell elongation and causes agravitropic phenotypes in wild-type roots (Sussman and Goldsmith 1981) (Table 1). As previously reported for *eir*

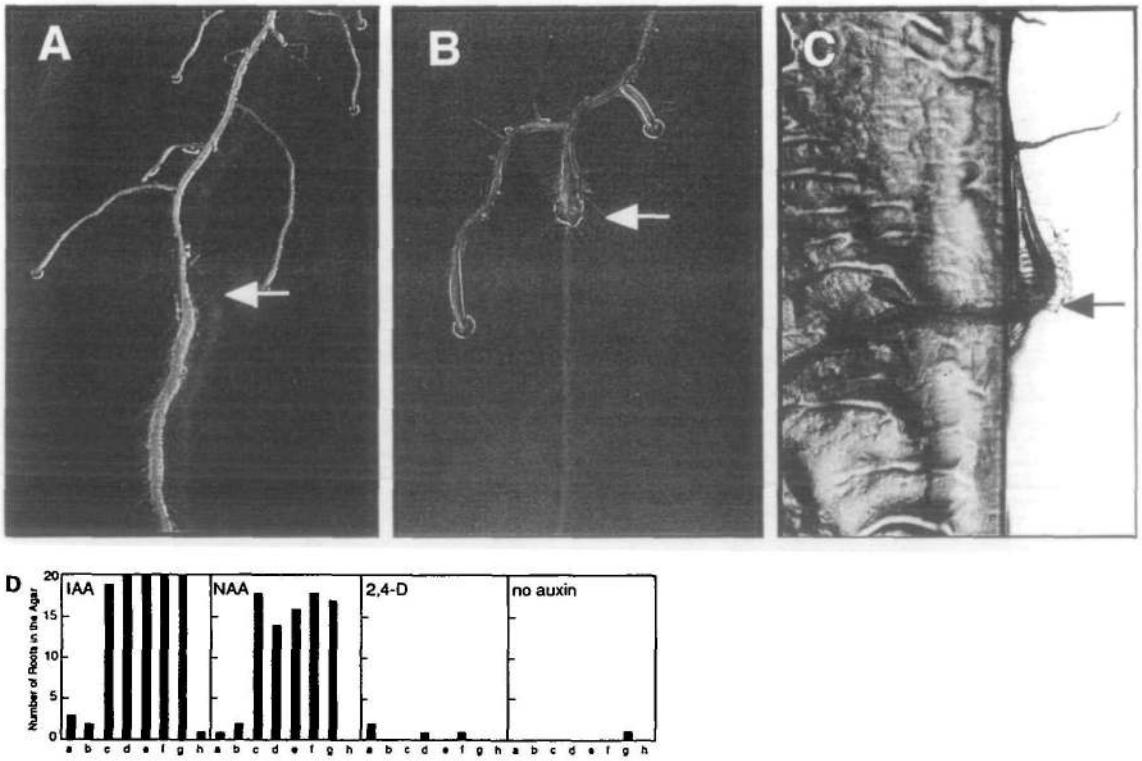

Fig. 2 Growth response of root tips on agar media containing auxins. Three-day-old seedlings grown as in Fig. 1 were transferred to the agar medium containing 33 nM IAA, 660 nM NAA, 10 nM 2,4-D, or no auxin, and grown on vertically oriented plates for a further 2 d under 16 h-light/8 h-dark illumination. Arrows indicate the position of the root tips at the time of transfer. (A) Wild-type Ler roots continued to grow on the surface of the agar medium containing 33 nM IAA. (B) *agr-2* root tips bend into the agar medium containing 33 nM IAA. (C) A side view of B. (D) Twenty roots were assayed for the bending response for each genotype per treatment. The number of main roots that bent into the agar medium was scored and shown in bar graph-form. a; Ler wild-type, b; Col wild-type, c; *agr-1*, d; *agr-2*, e; *agr-3*, f; *wav6-52*, g; *eir1-1*, and h; *aux1-7*.

Downloaded from https://academic.oup.com/pcp/article/39/10/1111/1844994 by guest on 20 August 2022

mutants, the root growth of all five *agr* alleles was more resistant than that of the wild type to 1-aminocyclopropane-1-carboxylic acid (ACC) which is converted to ethylene in planta (Table 1).

Although the auxin response of root growth was not different between wild types and *agr* mutants, *agr* roots did show a characteristic bending phenotype toward the auxin-containing agar medium. When seedlings were transferred

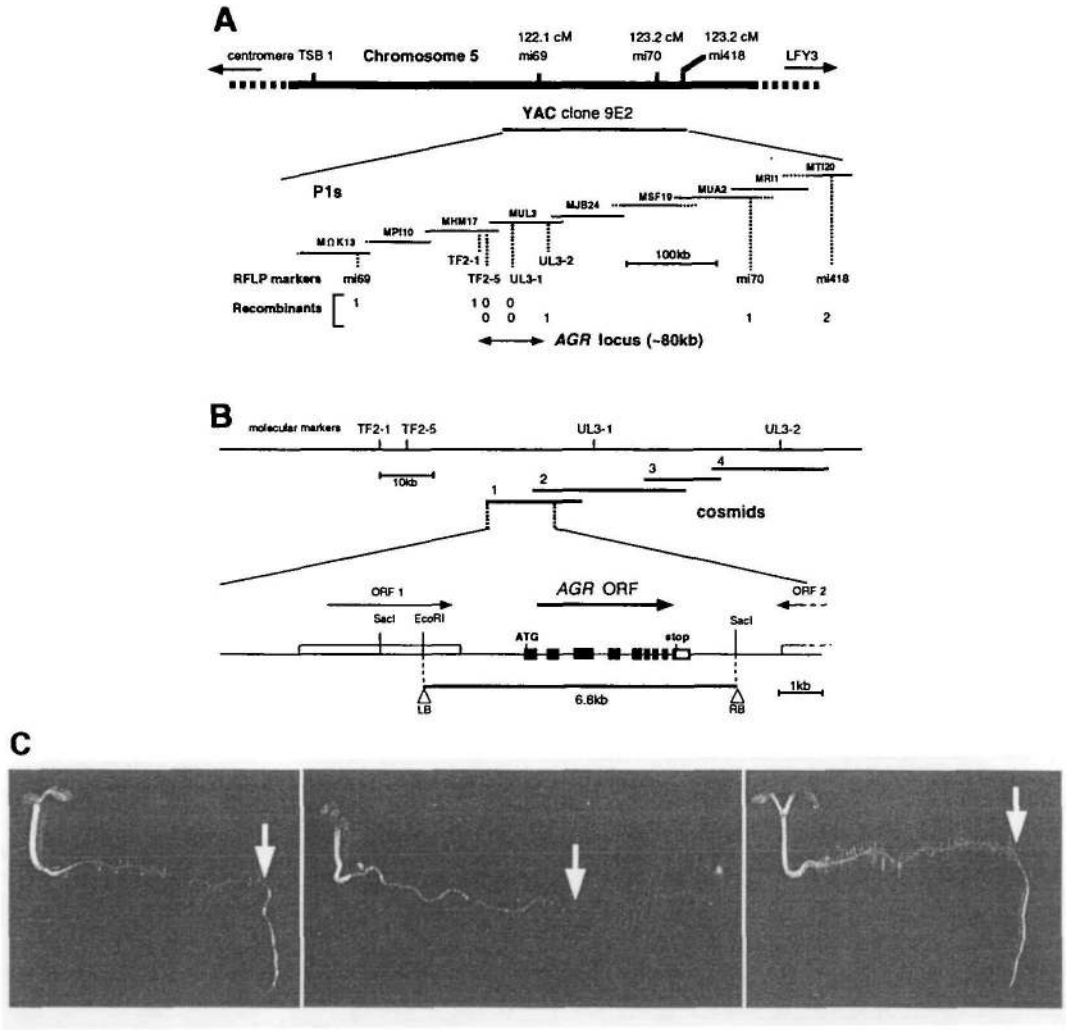

Fig. 3 Map-based cloning of *AGR*. (A) *wav6-52* (Ler) was crossed to the Col wild type, and DNAs from F2 *agr* seedlings were prepared for RFLP and PCR analysis as described (Dellaporta et al. 1983). YAC clone 9E2 was identified after screening the CIC YAC library (Creusot et al. 1995) using RFLP markers mi69, mi70, and mi418 as hybridizations probes. Standard methods for the growth of yeast, hybridization conditions, and YAC analysis were used (Rose et al. 1990, Ward and Jen 1990). A contig of 9 P1 clones covering the region between mi69 and mi418 was constructed after screening the Arabidopsis genomic P1 library (Liu et al. 1995). The information on the CAPS markers generated during the fine mapping (Shikanai et al. 1996) will appear on the AtDB web site (http://genome-www.stanford.edu/Arabidopsis/aboutcaps.html). The *wav6-52* allele has a polymorphism at UL3-2 (5′-CTCTAAG, instead of 5′-CTCTCAG in the Ler wild type), and this polymorphism was detected by direct sequencing of the genomic PCR products. Recombination break point analysis indicated that *AGR* is located between TF2-1 and UL3-2. (B) An Arabidopsis sub-genomic library was made from MUL3 in a binary cosmid vector pOCA28 (c.f. Olszewski et al. 1988). Four overlapping cosmid clones were screened and introduced into *eir1-1* plants by a vacuum infiltration protocol (Bent 1994). Cosmid 1 rescued the agravitropic phenotype of *eir1-1* roots, and the corresponding wild-type genomic sequence was obtained (http://www.kazusa.or.jp/arabi/chr5/status/released.html). Direct sequencing of the two genes located on the left side of cosmid 1, after PCR amplification from the *eir1-1* genome, detected a mutation (see text) in the putative *AGR* gene consisting of 9 exons. The 6.8-kb *Eco*RI-*Sac*I wild-type DNA fragment containing this gene was cloned into the pBI101 plant transformation vector, and introduced into *eir1-1* plants as above. The other gene was predicted to encode a homolog of extensin (ORF1). (C) Complementation of the *eir1-1* mutation by a binary vector containing the *AGR* gene. After the seedlings were grown for 3 d under light, the agar plates were rotated to the angle of 90° and then grown in the dark for one more day. Arrows indicate the position of the root tips at the time of rotation. Left to right: Col wild type, *eir1-1*, and *eir1-1* transformed with the 6.8-kb wild-type *AGR* gene.

Downloaded from https://academic.oup.com/pcp/article/39/10/1111/1844994 by guest on 20 August 2022

onto the agar surface of vertically oriented agar medium containing IAA, NAA, or 2,4-D, wild-type roots continued to grow downward on the agar surface (Fig. 2A, D). At high auxin concentrations, root growth on the surface was inhibited but still apparent. All five *agr* roots, however, grew into the agar medium containing 33 nM IAA or 660 nM NAA (Fig. 2B, C, D). Notably, 2,4-D tested at concentrations between 10 and 100 nM caused neither wild-type nor *agr* roots to grow into the 2,4-D-containing agar (Fig. 2D), and higher 2,4-D concentrations severely inhibited root growth. This bending response does not simply result from the agravitropic nature of *agr* roots, since *aux1* agravitropic roots which are presumably defective in auxin uptake (Bennet et al. 1996) do not show similar bending phenotypes (Fig. 2D). Because IAA and NAA are preferentially transported out of cultured tobacco cells through an auxin efflux carrier, while 2,4-D largely diffuses out (Delbarre et al. 1996), this bending phenotype of the *agr* roots may indicate that a reduction in AGR function interferes with the carrier-mediated efflux of exogenously-supplied auxin.

Positional cloning of the AGR gene—We mapped *AGR* to the bottom of chromosome 5 between the molecular markers mi69 (122.1 cM) and mi70 (123.2 cM). A yeast artificial chromosome (YAC) clone, 9E2, with a 580-kb insert, hybridized to mi69 and mi70 probes, and also to a neighboring marker, mi418 (123.2 cM). A contiguous map (contig) of overlapping P1s covering YAC 9E2 was constructed (Fig. 3A). Fine-scale restriction fragment length polymorphism (RFLP) analysis of *agr* recombinants indicated that the *AGR* gene was located in an approximately 80-kb region flanked by the molecular marker TF2-1 in P1 clone MHM17 and UL3-2 in MUL3.

An overlapping cosmid contig covering MUL3 was made, and these cosmids were introduced into the *eir1-1* mutant (Fig. 3B). Only cosmid 1 rescued the agravitropic defect of *eir1-1* roots (data not shown). Sequence data from the cosmid 1 region revealed that two intact open reading frames (ORFs) were present on the left side of cosmid 1 but not in an overlapping cosmid 2. Genomic sequencing of these two candidate genes in *eir1-1* identified a mutation at a splicing acceptor site in one of the candidates (see below for details). The 6.8-kb wild-type genomic fragment containing this putative *AGR* gene was introduced into the *eir1-1* mutant. T1 and T2 kanamycin-resistant seedlings containing the transgene had a root growth phenotype identical with the wild type (Fig. 3C), demonstrating that this is the *AGR* gene.

AGR encodes a novel membrane-protein family member with limited homologies to bacterial transporters—The longest cDNA obtained was 2,232 nt long, and contained a predicted ORF encoding a 647 amino acid 69.3 kDa protein (Fig. 4). Comparison of the predicted amino acid sequence with sequences in GenBank identified several highly homologous sequences in the Arabidopsis genome. Three such homologs found in database entries from the *Arabidopsis* Genome Initiative were referred to as *AEH1* (for *Arabidopsis EIR1 Homolog*), *AEH2*, and *AEH3*, according to the nomenclature used by Luschnig et al. (1998). *AEH1* and *AEH3* are located at 31.9 cM and 114.23 cM on chromosome 1, whereas *AEH2* is at 33.26 cM on chromosome 5. No phenotypically identified mutants map at these genomic regions. Mutants with altered responses to auxin transport inhibitors (*tir1* to *tir7*; Ruegger et al. 1997) do not correspond to the defects in the three *AEH* genes either (M. Estelle, and our unpublished results). There are several other homologous sequences in the Arabidopsis and rice expressed sequence tag (EST) databases (data not shown). In total, there are at least five *AEH* genes in Arabidopsis. No close homologs were found in DNA databases other than from plants, indicating that *AGR* and its homologs form a novel protein family specific to plants.

Alignment and hydrophobicity analyses (Fig. 4 and data not shown) of the predicted amino acid sequences of *AGR*, *AEH1*, *AEH2*, and *AEH3* show that the amino and carboxyl terminal regions are homologous. The central hydrophilic regions are divergent, and AEH2 even lacks the entire central hydrophilic region. Five membrane-spanning regions were identified in each of the amino and carboxyl termini of these four proteins. Computer-assisted motif search PSORT (http://psort.nibb.ac.jp:8800/helpwww.html) predicted a potential amino-terminal signal peptide that may be cleaved after Ser^{61}, although this cleavage would remove the first two transmembrane domains which are highly conserved among the AEHs. Similar computer searches did not predict amino-terminal signal peptides for AEH2 and AEH3. Several integral membrane proteins do not possess amino-terminal signal peptides (Dalbey et al. 1995). Therefore, the putative signal cleavage site predicted for AGR may not actually be used. Several potential *N*-glycosylation sites are present in these sequences (data not shown).

The conserved transmembrane regions at the amino and carboxyl termini show limited similarity to several bacterial membrane proteins, and the amino acid sequence of a representative bacterial transporter mdcF is aligned in Fig. 4. The *mdcF* gene is a member of the malonate operon, and is predicted to function as a malonate transporter (Hoenke et al. 1997). The homologies to bacterial transporters suggest that AGR may function as a membrane-localized transporter.

Molecular analysis of agr mutations—Molecular defects in the five *agr* alleles were determined by sequencing the PCR-amplified *AGR* locus from the mutant genomes (Fig. 4). Missense mutations caused a Gly^{539} to Asp substitution in the strong allele *agr-1*, and a Gly^{541} to Glu substitution in *wav6-52*. These two glycine residues in a transmembrane domain are strictly conserved in AEH1, AEH2,

Downloaded from https://academic.oup.com/pcp/article/39/10/1111/1844994 by guest on 20 August 2022

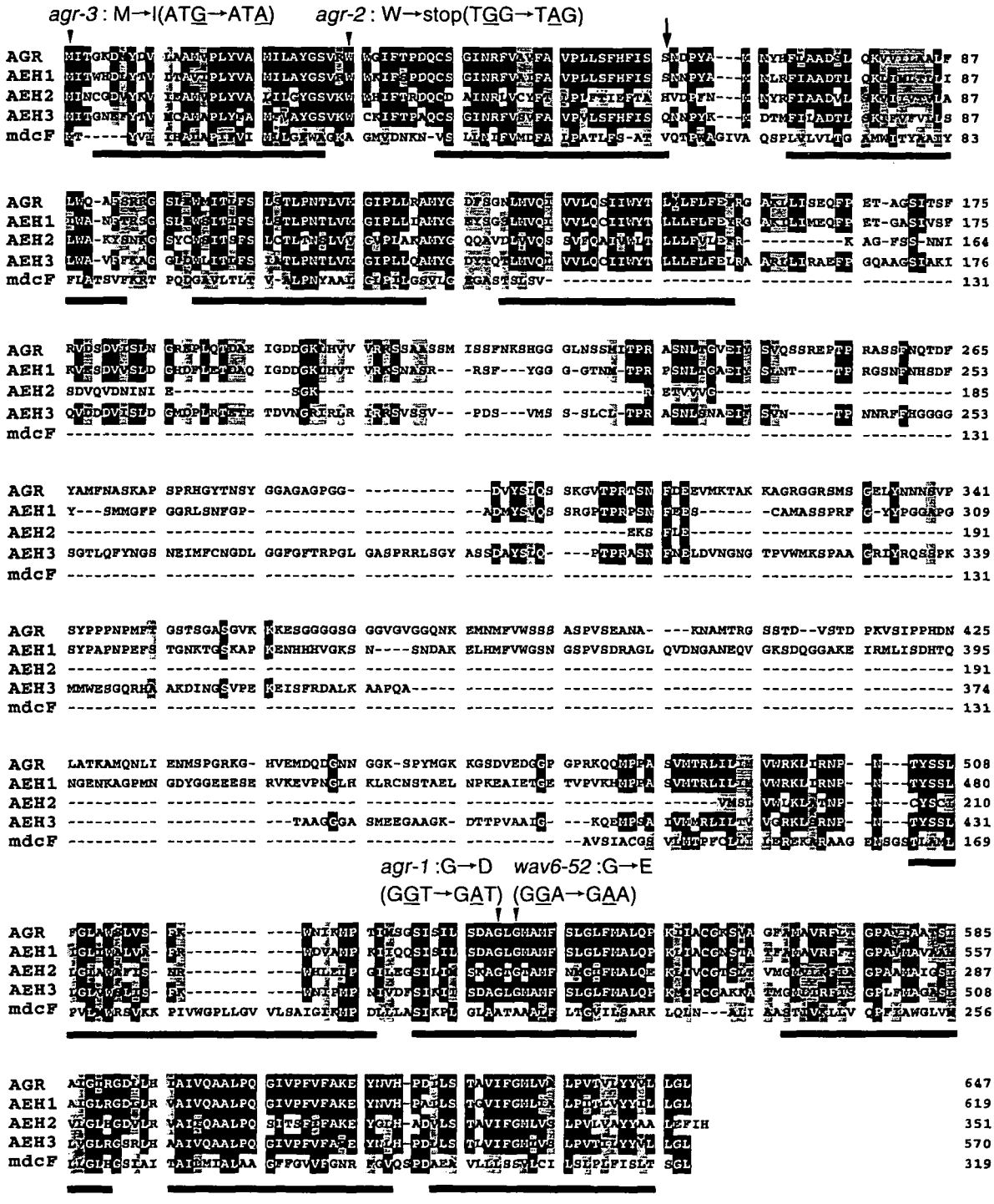

Fig. 4 Alignment of deduced amino acid sequences of *AGR*, the three putative homologs AEH1, AEH2, and AEH3, and a probable bacterial transporter mdcF. Residues are boxed to indicate amino acid identity (in black boxes) or functional conservation (in shaded boxes; L, I, V, M; A, S, T; F, W, Y; N, Q; D, E; and K, R). *AGR* cDNAs were cloned by 5′-RACE and 3′-RACE from wild-type root RNA (ecotype Ler). The AEH sequences were deduced from the genomic sequences by predicting the probable splice sites. Black lines below the mdcF sequence correspond to the 10 potential transmembrane domains shared by all five proteins. An arrow indicates the potential cleavage site for an *N*-terminal signal peptide in AGR (see text). Mutations in the four *agr* alleles are also indicated above the AGR sequence (mutated bases are underlined).

Downloaded from https://academic.oup.com/pcp/article/39/10/1111/1844994 by guest on 20 August 2022

and AEH3 (Fig. 4), and also in two AEH proteins encoded by partial Arabidopsis ESTs (35D8T7 and 121L8T7; data not shown). In *agr-2*, Trp^{30} was mutated to a stop codon, thus terminating translation prematurely. In the *agr-3* allele, Ile was substituted for the translation initiator Met. Since *agr-3* is a weak allele, a downstream methionine (e.g. Met^{7}) might instead be used for translation initiation. The molecular defect in *eir1-1* was a G to A transition in the absolutely conserved 3′ splice junction in intron 5, as reported by Luschnig et al. (1998). PCR primers designed from the amino- and carboxyl-terminal domains of AGR, however, amplified wild-type levels of *AGR* cDNA after reverse transcription (RT)-PCR from *eir1-1* root RNA (data not shown). Sequencing of the RT-PCR product revealed that the splice junction in *eir1-1* (caagTG; the mutated base is underlined) was shifted downstream by one base relative to the wild-type junction (cagGTG). This alteration in the splice site is expected to cause a frame-shift within the *AGR* ORF, resulting in a truncated AGR protein in which the carboxy terminal 129 amino acid residues are replaced by 3 amino acid residues. Since *eir1-1* roots show weak gravitropic response, the truncated AGR protein may still retain residual AGR activity.

Expression of AGR and its homologs—PCR primers were designed from the amino- and carboxyl-terminal sequences that are specific to *AGR* and the three *AEH*s. RT-PCR analysis of various Arabidopsis organs detected specifically amplified DNA fragments of the expected size for each pair of PCR primers (Fig. 5). PCR amplification of Arabidopsis genomic DNA produced DNA fragments of larger sizes due to the introns in the central regions (data not shown), indicating that our RT-PCR analysis detected amplification from RNA. Representative RT-PCR products were partially sequenced and found to match the DNA sequences of the expected genes (data not shown), indicating that the PCR conditions specifically amplified the intended sequences. The RT-PCR analysis showed that *AGR* is specifically expressed in the root. The expression of *AEH1* appears to be constitutive. *AEH2* is mostly expressed in the whole stem and very weakly in the flower, whereas *AEH3* is expressed in the root, and the upper part of the stem which includes elongating tissues (but not in the lower part of the stem without elongating tissues), and weakly in the flower.

We have cloned the Arabidopsis *Agravitropic* locus gene *AGR* and showed that AGR is a root-specific member of a novel membrane protein family. The similarity of the membrane-spanning domains of AGR and its homologs to several bacterial membrane transporters, and the bending response of *agr* root tips into agar medium containing auxins which are transported by the efflux carrier, suggest that AGR (and possibly other members of this family) may function as an auxin transporter. While this manuscript was in preparation, Luschnig et al. (1998) reported the cloning of

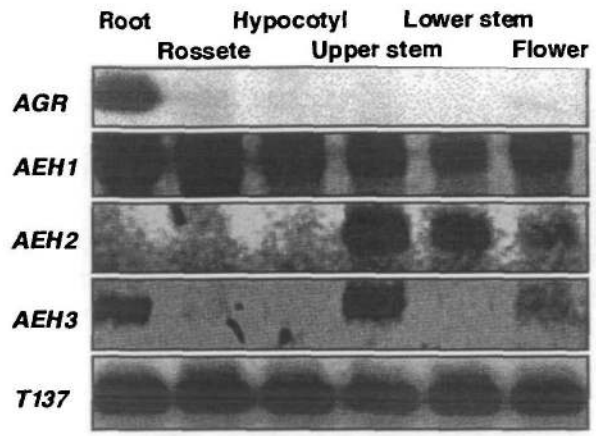

Fig. 5 RT-PCR expression analysis of *AGR* and its homologs in wild-type plants. Gene-specific PCR primers were designed and used to amplify total RNA by RT-PCR from root and hypocotyl of seedlings, and rosette leaf, upper stem, lower stem, and flower of mature plants. PCR products were blotted onto membrane filters and hybridized with ^{32}P-labeled gene-specific DNA probes. As an amplification control, the *T137* gene that is constitutively expressed in all Arabidopsis organs (An et al. 1996) was used. PCR conditions were: 30 s at 94°C, 30 s at 57°C, and 1 min at 72°C, for 40 cycles. PCR-primers used were: 5′-AAGAATGCTATGACAAGAGG and 5′-AACATAGCCATTCCAAGACC for *AGR*, 5′-CAATATGATCACATGGCACG and 5′-TGAAGAGCTTATAGCCCGAG for *AEH1*, 5′-AACCATGATAAATTGTGGAG and 5′-ACTCCAGAGCTGCGTAGTAG for *AEH2*, 5′-AAAGATGATAACGGGAAACG and 5′-GTTGTGTGAATCATAGGCCC for *AEH3*, and 5′-GTTCCCAACTTCCTCTTAGCAA and 5′-CTTCTTTTGTCTGAACCACCGCA for *T137*.

AGR (referred in their paper as *EIR1*) from a transposon-tagged allele *eir1-3*, and gave several additional lines of evidence that AGR may be the auxin efflux carrier: *agr* roots are insensitive to an elevated level of endogenous auxin, and fail to induce an auxin-inducible gene in the expansion zone; and expression of AGR in yeast confers resistance to fluorinated indolic compounds. Increased resistance of *agr* root growth to ethylene suggests a possible interplay between auxin and ethylene in root gravitropism. Analysis of double mutants have shown that *agr* partially suppresses the inhibition of root growth by the ethylene mutants, *ctr1* and *eto3* (Roman et al. 1995, Luschnig et al. 1998), and *agr* is defective in the ACC-induced expression of an auxin-responsive promoter in roots (Luschnig et al. 1998). It has also been reported that the ethylene-insensitive mutant *ein2* and the root-specific auxin-resistant and agravitropic mutant *aux1* are both resistant to ethylene and the auxin-transport inhibitors, *N*-1-naphtylphtalamic acid and TIBA (Hobbie and Estelle 1994, Fujita and Syono 1996). In etiolated pea stem briefly exposed to red light, ethylene was proposed to inhibit the lateral migration of IAA in response to gravity (Kang and Burg 1972). Taken together, ethylene may inhibit active auxin transport, for which

Downloaded from https://academic.oup.com/pcp/article/39/10/1111/1844994 by guest on 20 August 2022

AGR is a critical component.

Auxin is thought to move in an acropetal direction through the stele of the root. In the root cap region, it has been proposed that auxin is transported laterally and then basipetally through the epidermal tissues to the elongation zone (Estelle 1996, Lomax et al. 1995). A modified version of the Cholodny-Went hypothesis states that auxin is distributed asymmetrically in the root cap upon gravistimulation and transported away from the root tip into the elongation zone, where cell elongation is inhibited at the lower side with a supra-optimal auxin level (Hasenstein and Evans 1986). According to this model, AGR may be localized at the basal side of each epidermal cell in the region between the root tip and the elongation zone. Root tip bending of *agr* mutant roots toward exogenous IAA and NAA (Fig. 2) might result from an accumulation of exogenously supplied auxin in the epidermis at the agar-facing side of the elongation zone, which is normally prevented by the pumping out of the exogenous auxin through the wild-type AGR function. Since 2,4-D is not transported by the efflux carrier and passively diffuses out of the cells (Delbarre et al. 1996), this synthetic auxin may not induce such root tip bending in either wild type or *agr* mutants. Immunohistochemical localization of AGR, or expression analysis of an epitope-tagged *AGR* gene in transgenic roots, should precisely define the cellular localization of AGR, and may clarify the existence of an AGR-mediated auxin flow in root gravitropism. Other members of the AGR/EIR1 family might also be involved in the transport of small molecules, including auxin. Since auxin is implicated in the regulation of various aspects of plant growth and development, such as cell expansion, apical dominance, vascular differentiation, lateral root development, phototropism and gravitropism, AGR homologs may be involved in auxin-regulated processes other than gravitropism and cell elongation. Characterization of AGR and other AGR/EIR1 members should advance our understanding of auxin-related plant processes.

We thank Drs. Padday Maher, Kiyotaka Okada, and Fred Ausubel for the three *agr* alleles, *wav6-52*, and the pOCA28 cosmid vector, respectively. *eir1-1*, *aux1-7*, and the CIC YAC library were obtained from the Arabidopsis Biological Resource Center, Ohio, U.S.A., and the Arabidopsis genomic P1 library was from the Mitsui Plant Biotechnology Institute. Yuko Watanabe and Hiroe Ohnishi were respectively acknowledged for the initial mapping work and Arabidopsis transformation. We would like to thank Dr. Daisuke Shibata of the Mitsui Plant Biotechnology Institute for his discussion and continued encouragement, and Dr. Robert Winz for the critical reading of the manuscript. K.U. was supported by a JSPS Research Fellowship for Young Scientists (No. 8628). This work was supported in part by a Grant-in-Aid for Scientific Research on Priority Areas ("The Molecular Basis of Flexible Organ Plans in Plants", No. 06278103) from the Ministry of Education, Science, Sports and Culture of Japan, to T. H.

References

An, Y.-Q., Huang, S., McDowell, J.M., McKinney, E.C. and Meagher, R.B. (1996) Conserved expression of the Arabidopsis *ACT1* and *ACT3* actin subclass in organ primordia and mature pollen. *Plant Cell* 8: 15–30.

Bell, C.J. and Maher, E.P. (1990) Mutants of *Arabidopsis thaliana* with abnormal gravitropic responses. *Mol. Gen. Genet.* 220: 289–293.

Bennett, M.J., Marchant, A., Green, H.G., May, S.T., Ward, S.P., Millner, P.A., Walker, A.R., Schulz, B. and Feldmann, K.A. (1996) *Arabidopsis AUX1* gene: a permease-like regulator of root gravitropism. *Science* 273: 948–950.

Bent, A. (1994) Transformation of Arabidopsis by vacuum infiltration. The Compleat Guide, http://genome-www.stanford.edu/Arabidopsis/comguide/chap_1_plants/9_vacuum_transformation.html.

Creusot, F., Fouilloux, E., Dron, M., Lafleuriel, J., Picard, G., Billault, A., Le Paslier, D., Cohen, D., Chabouté, M.-E., Durr, A., Fleck, J., Gigot, C., Camilleri, C., Bellini, C., Caboche, M. and Bouchez, D. (1995) The CIC library: a large insert YAC library for genome mapping in *Arabidopsis thaliana*. *Plant J.* 8: 763–770.

Dalbey, R.E., Kuhn, A. and von Heijne, G. (1995) Directionality in protein translocation across membranes: the N-tail phenomenon. *Trends Cell Biol.* 5: 380–383.

Delbarre, A., Muller, P., Imhoff, V. and Guern, J. (1996) Comparison of mechanisms controlling uptake and accumulation of 2,4-dichlorophenoxy acetic acid, naphthalene-1-acetic acid, and indole-3-acetic acid in suspension-cultured tobacco cells. *Planta* 198: 532–541.

Dellaporta, S., Wood, J. and Hicks, J. (1983) A plant DNA minipreparation: version II. *Plant Mol. Biol. Rep.* 1: 19–21.

Evans, M.L. (1991) Gravitropism: interaction of sensitivity modulation and effector redistribution. *Plant Physiol.* 95: 1–5.

Estelle, M. (1996) Plant tropisms: the ins and outs of auxin. *Curr. Biol.* 6: 1589–1591.

Fujita, H. and Syono, K. (1996) Genetic analysis of the effects of polar auxin transport inhibitors on root growth in *Arabidopsis thaliana*. *Plant Cell Physiol.* 37: 1094–1101.

Hasenstein, H. and Evans, M.L. (1986) Calcium dependence of rapid auxin action in maize roots. *Plant Physiol.* 81: 439–443.

Haughn, G.W. and Somerville, C. (1986) Sulfonylurea-resistant mutants of *Arabidopsis thaliana*. *Mol. Gen. Genet.* 204: 430–434.

Hobbie, L. and Estelle, M. (1994) Genetic approaches to auxin action. *Plant Cell Environ.* 17: 119–127.

Hoenke, S., Schmid, M. and Dimroth, P. (1997) Sequence of a gene cluster from *Klebsiella pneumoniae* encoding malonate decarboxylase and expression of the enzyme in *Escherichia coli*. *Eur. J. Biochem.* 246: 530–538.

Kang, B.G. and Burg, S.P. (1972) Relation of phytochrome-enhanced geotropic sensitivity to ethylene production. *Plant Physiol.* 50: 132–135.

Liu, Y.-G., Mitsukawa, N., Vazques-Tello, A. and Whittier, R.F. (1995) Generation of a high-quality P1 library of *Arabidopsis* suitable for chromosome walking. *Plant J.* 7: 351–358.

Lomax, T.L., Muday, G.K. and Rubery, P.H. (1995) Auxin transport. *In* Plant Hormones. Edited by Davies, P.J., pp. 509–530. Kluwer Academic Publishers, Dordrecht.

Luschnig, C., Gaxiola, G.A., Grisafi, P. and Fink, G.R. (1998) EIR1, a root-specific protein involved in auxin transport, is required for gravitropism in *Arabidopsis thaliana*. *Genes & Dev.* 12: 2175–2187.

Okada, K. and Shimura, Y. (1990) Reversible root tip rotation in *Arabidopsis* seedlings induced by obstacle-touching stimulus. *Science* 250: 274–276.

Olszewski, N.E., Martin, F.B. and Ausubel, F.M. (1988) Specialized binary vector for plant transformation: expression of the *Arabidopsis thaliana* AHAS gene in *Nicotiana tabacum*. *Nucl. Acids Res.* 16: 10765–10782.

Roman, G., Lubarsky, B., Kieber, J.J., Rothenberg, M. and Ecker, J.R. (1995) Genetic analysis of ethylene signal transduction in *Arabidopsis thaliana*: five novel mutant loci integrated into a stress response pathway. *Genetics* 139: 1393–1409.

Rose, M., Winston, F. and Hieter, P. (1990) *Methods in Yeast Genetics: a Laboratory Course Manual*. Cold Spring Harbor Laboratory Press,

Downloaded from https://academic.oup.com/pcp/article/39/10/1111/1844994 by guest on 20 August 2022

New York.
Ruegger, M., Dewey, E., Hobbie, L., Brown, D., Bernasconi, P., Turner, J., Muday, G. and Estelle, M. (1997) Reduced naphthylphthalamic acid binding in the *tir3* mutant of Arabidopsis is associated with a reduction in polar auxin transport and diverse morphological defects. *Plant Cell* 9: 745–757.
Sack, F.D. (1991) Plant gravity sensing. *Int. Rev. Cytol.* 127: 193–252.
Shikanai, T., Utsuno, K., Hashimoto, T. and Yamada, Y. (1996) Construction of PCR-based CAPS markers for rapid genome mapping. *Plant Tissue Culture Lett.* 13: 91–95.
Sussman, M.R. and Goldsmith, M.H.M. (1981) The action of specific inhibitors of auxin transport on uptake of auxin and binding of *N*-1-naphtylphtalamic acid to a membrane site in maize coleoptyles. *Planta* 153: 13–18.
Ward, E. and Jen, G. (1990) Isolation of single-copy-sequence clones from a yeast artificial chromosome library of randomly-sheared *Arabidopsis thaliana* DNA. *Plant Mol. Biol.* 14: 561–568.

(Received September 4, 1998; Accepted September 21, 1998)

Downloaded from https://academic.oup.com/pcp/article/39/10/1111/1844994 by guest on 20 August 2022